American Mineralogist, Volume 75, pages 256–261, 1990

Molecular orbital (SCF-Xα-SW) theory of Fe^{2+}-Mn^{3+}, Fe^{3+}-Mn^{2+}, and Fe^{3+}-Mn^{3+} charge transfer and magnetic exchange in oxides and silicates

David M. Sherman
U.S. Geological Survey, M.S. 964, Box 25046, Denver Federal Center, Denver, Colorado 80225, U.S.A.

Abstract

Metal-metal charge-transfer and magnetic exchange interactions have important effects on the optical spectra, crystal chemistry, and physics of minerals. Previous molecular orbital calculations have provided insight on the nature of Fe^{2+}-Fe^{3+} and Fe^{2+}-Ti^{4+} charge-transfer transitions in oxides and silicates. In this work, spin-unrestricted molecular orbital calculations on $(FeMnO_{10})$ clusters are used to study the nature of magnetic exchange and electron delocalization (charge transfer) associated with Fe^{3+}-Mn^{2+}, Fe^{3+}-Mn^{3+}, and Fe^{2+}-Mn^{3+} interactions in oxides and silicates.

The calculated relative energies of the Fe($3d$) and Mn($3d$) orbitals indicate that the formal charge configuration Fe^{2+}-Mn^{3+} is unstable relative to the configuration Fe^{3+}-Mn^{2+}. Hence, Mn^{3+} cannot exist in silicates in which Fe^{2+} occurs in an edge-sharing polyhedron. The energy for optically induced $Mn^{2+} \rightarrow Fe^{3+}$ charge transfer is estimated to be 14900 cm^{-1}. The energy for $Mn^{3+} \rightarrow Fe^{3+}$ charge transfer is estimated to be 17800 cm^{-1}. Jahn-Teller distortion of the Mn^{3+} site will increase this energy. Because of their energies, absorption bands due to Mn-Fe charge transfer will be difficult to resolve from bands due to the ligand-field transitions of Fe^{3+}, Mn^{2+}, and Mn^{3+}.

Both the Fe^{3+}-Mn^{2+} and Fe^{3+}-Mn^{3+} interactions are found to be antiferromagnetic. The calculated exchange constants, however, are probably greatly overestimated.

Introduction

This paper is the third in a series of investigations on metal-metal charge-transfer and magnetic exchange interactions in minerals (Sherman, 1987a, 1987b). Metal-metal charge-transfer transitions are of fundamental interest because they provide a mechanism for semiconduction and redox reactions in the solid state. It is also now realized that metal-metal charge-transfer and magnetic-exchange interactions greatly affect the optical (visible to near-infrared) spectra of Fe- and Mn-bearing minerals. In two previous papers (Sherman, 1987a, 1987b) the nature of $Fe^{2+} \rightarrow Fe^{3+}$ and $Fe^{2+} \rightarrow Ti^{4+}$ charge transfer was investigated using spin-unrestricted self-consistent field–Xα–scattered wave (SCF-Xα-SW) molecular orbital calculations on $(Fe_2O_{10})^{15-}$ and $(FeTiO_{10})^{14-}$ clusters. Those calculations show that weak metal-metal bonding is what allows the optically and thermally induced charge-transfer transitions. It was also found that the weak metal-metal bonding induces ferromagnetic coupling between Fe^{2+} and Fe^{3+} cations. This result is in agreement with Zener's double-exchange model and empirical evidence on the magnetic structures of mixed-valence minerals (e.g., Coey and Ghose, 1988).

In this paper, the possible interactions between Fe and Mn cations will be investigated using SCF-Xα-SW calculations on the electronic structures of $(FeMnO_{10})^{n-}$ clusters. Fe-Mn interactions are of particular interest because many iron silicates and oxides contain substantial amounts of manganese. Within the redox conditions of the Earth's crust, both metals exist in several oxidation states (e.g., Fe^{2+}, Fe^{3+}, Mn^{2+}, Mn^{3+}, Mn^{4+}). A number of interesting possibilities arise, therefore, regarding the crystal chemistry, spectra, and electronic structures of Fe-Mn solid solutions. It is not clear whether Fe^{2+} and Mn^{3+} cations can coexist in a structure or if only Fe^{3+}-Mn^{2+} and Fe^{3+}-Mn^{3+} pairs are stable. Optically, or perhaps thermally, induced charge-transfer transitions between Fe and Mn (e.g., $Fe^{2+} \rightarrow Mn^{3+}$, $Mn^{3+} \rightarrow Fe^{3+}$, $Mn^{2+} \rightarrow Fe^{3+}$) seem physically reasonable, yet the energies of such transitions are unknown. The nature of the magnetic coupling or exchange interactions between Fe and Mn cations is of interest insofar as Mn may affect the Mössbauer spectra and magnetochemistry of iron oxides and silicates (e.g., Vandenberghe et al., 1986).

Computational parameters

The geometry of the $(FeMnO_{10})^{n-}$ clusters is shown in Figure 1. The symmetry of each cluster is C_{2v} (2 mm). The theory of the SCF-Xα-SW method is described by Johnson (1973) but will be outlined here: The $(FeMnO_{10})^{n-}$ cluster is partitioned into a set of overlapping spheres corresponding to the Fe, Mn, and O atoms. The cluster is surrounded by an outer sphere, and to stabilize the charged cluster, a Watson sphere (with charge $n+$) is used. An initial potential for the cluster is obtained by superpositioning the charge densities of free Fe^0, Mn^0, and $O^{-1.5}$

ions. Within the atomic and outer spheres, the potential is spherically averaged; in the intersphere region, the potential is volume-averaged to give a constant value. The Schrödinger equation [with the exchange term given by the $X\alpha$ approximation (Slater, 1974)] is solved within each region, and the solutions are matched at the sphere boundaries. From the new one-electron wave functions, a new potential is generated, and the procedure is repeated. About 20–30 iterations are needed to obtain a self-consistent calculation. The most important adjustable parameters in the method are the atomic sphere radii. These were chosen using the overlapping sphere approach of Norman (1976). The atomic α values were taken from Schwarz (1972). The Fe-O and Mn-O bond lengths used were obtained from the Shannon and Prewitt (1969) ionic radii.

Results and discussion

Fe^{3+}-Mn^{2+} and Fe^{2+}-Mn^{3+} interactions

The electronic structure of the $(FeMnO_{10})^{14-}$ cluster with Fe-O and Mn-O bond lengths of 2.00 and 2.16 Å, respectively, is shown in Figures 2a and 2b. The orbitals within the O(2*p*) band are Mn-O and Fe-O bonding and O(2*p*) nonbonding. In the molecular orbital diagrams, the O(2*p*) orbitals are not shown explicitly, but their energy ranges are indicated by the shaded regions. The nature of the Fe-O and Mn-O bonds and the electronic structures of simple FeO_6 and MnO_6 coordination polyhedra are given in Sherman (1984) and Sherman (1985). What is of primary interest here is the relative energies of the Mn(3*d*)- and Fe(3*d*)-like molecular orbitals. These are Mn-O or Fe-O antibonding. Octahedral coordination causes the five 3*d* orbitals of a transition-metal cation to be split into a threefold degenerate t_{2g} set and a twofold degenerate e_g set. The energy difference between the t_{2g} and e_g set is the crystal-field splitting. Each *d*-orbital set is split, in turn, into its spin-up and spin-down counterparts. Hence, in the $(FeMnO_{10})^{n-}$ clusters, there are eight sets of *d* orbitals corresponding to the spin-up and spin-down Mn e_g and t_{2g} sets together with the spin-up and spin-down Fe e_g and Fe t_{2g} sets. In the $FeMnO_{10}$ cluster, the orbitals within each e_g or t_{2g} set are nondegenerate because of weak Fe-Mn bonding or antibonding interactions. Because of these weak metal-metal bonding interactions, the *d* orbitals of transition-metal cations may give rise to narrow bands in a solid instead of discrete levels as in a simple complex.

From the orbital occupancies and charge distributions, the Fe and Mn atoms are unambiguously in the Fe^{3+} and Mn^{2+} oxidation states. In both the ferromagnetic and antiferromagnetic configurations, there is some weak *d*-electron delocalization over the two metal atoms through Fe(t_{2g})-Mn(e_g) and Fe(e_g)-Mn(t_{2g}) overlap across the shared edge (the Fe-Mn bonding and antibonding interactions). The highest-energy occupied orbital is shown in Figure 3. This is a Mn(e_g) orbital that is Fe-Mn antibonding. Because both the Fe-Mn bonding and antibonding orbitals are filled, there is no net Fe-Mn bond. That is to be contrasted with the situation found for the Fe^{2+}-Fe^{3+} pair in the $(Fe_2O_{10})^{15-}$ clusters (Sherman, 1987a). There, a net Fe-Fe bonding interaction results from the *d*-orbital overlap provided that the Fe^{2+} and Fe^{3+} cations are ferromagnetically coupled (this is the "double-exchange" mechanism described by Zener). The absence of Fe^{3+}-Mn^{2+} bonding precludes ferromagnetic coupling by double ex-

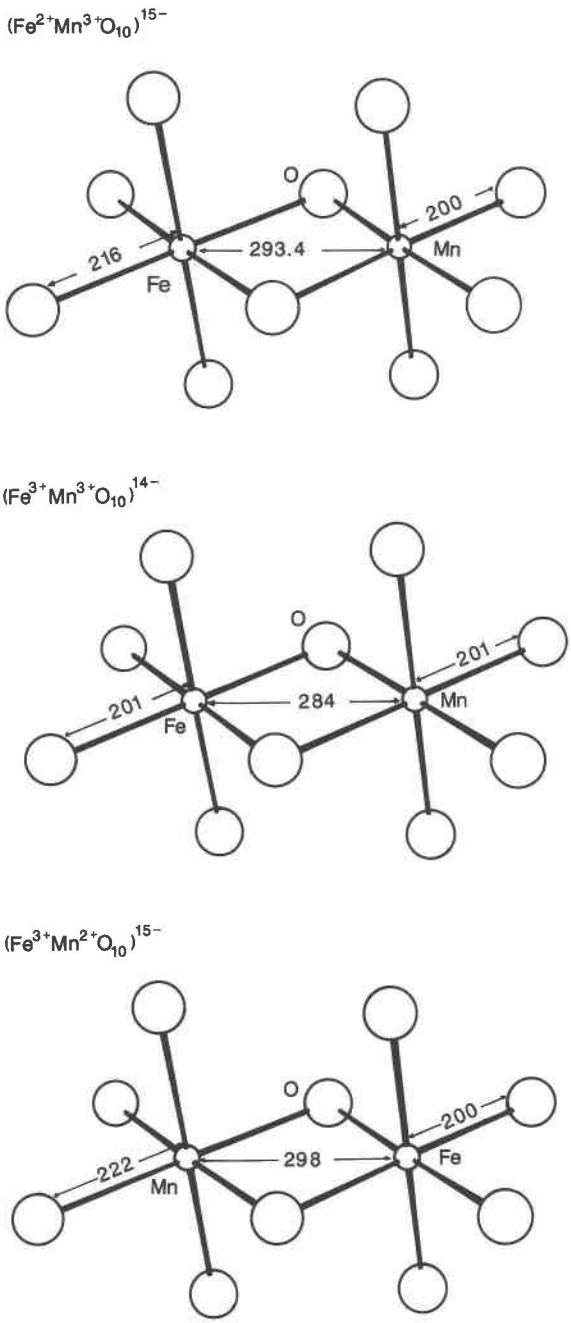

Fig. 1. Structures and bond lengths (in Å × 10^2 used in the $FeMnO_{10}$ clusters. The bond lengths were obtained from the sum of the Shannon and Prewitt (1969) ionic radii.

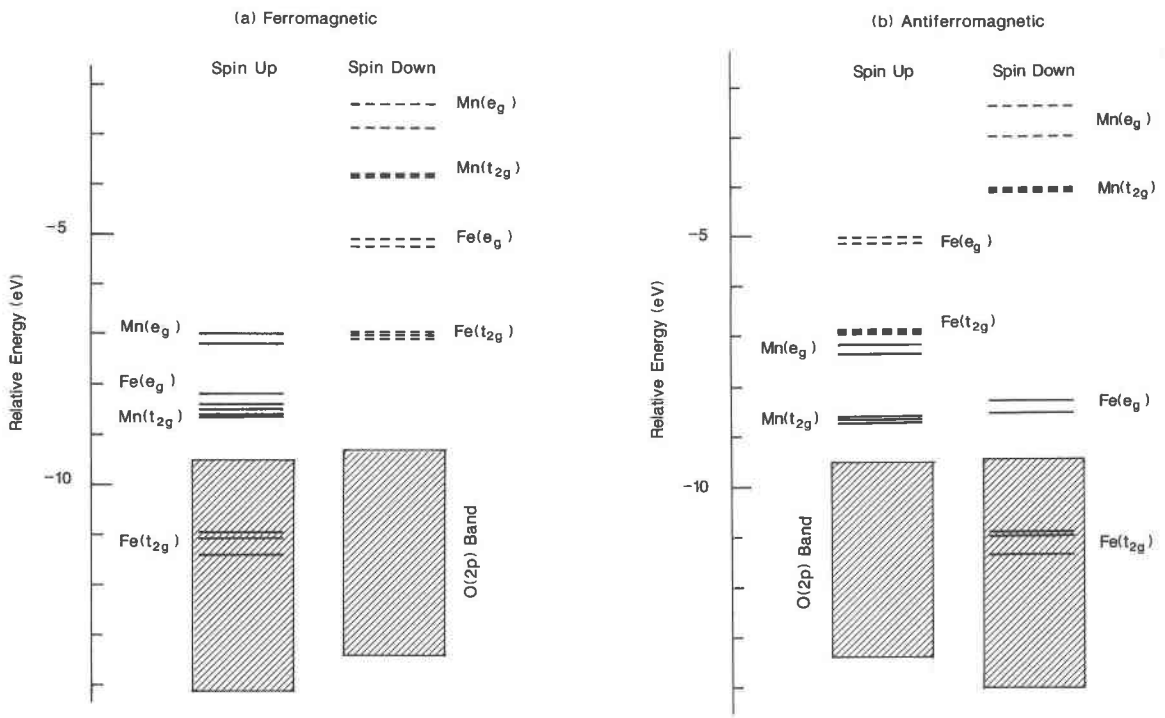

Fig. 2. Molecular orbital diagram for the $Fe^{3+}Mn^{2+}O_{10}$ cluster in the (a) ferromagnetic and (b) antiferromagnetic configurations. Orbitals indicated with a dashed line are unoccupied. Note that the orbital energies correspond to "orbital electronegativities" (Slater, 1974). The energy differences between orbitals in a given configuration do not necessarily correspond to electronic transition energies. For example, the spin-up Mn(e_g) and spin-down Fe(t_{2g}) orbitals are nearly degenerate in the MO diagram; however, the energy for the Mn(e_g) → Fe(t_{2g}) transition is found to be 14900 cm^{-1}. As an electron is transferred from one orbital to another, the orbital energies will "relax" about the new electronic configuration. To account for the orbital relaxation, electronic transition energies must be calculated using the transition-state formalism of Slater (1974).

change. In fact, the energy-level diagrams in Figure 2 imply that the antiferromagnetic configuration is the ground state according to Fermi statistics (in the ferromagnetic configuration, unoccupied orbitals lie below occupied orbitals). Antiferromagnetic coupling is found for Fe^{3+}-Fe^{3+} pairs, which are isoelectronic with Fe^{3+}-Mn^{2+}. The antiferromagnetic coupling can be modeled by using the Heisenberg Hamiltonian:

$$H = -J_{ab}\mathbf{S}_a\mathbf{S}_b$$

where J_{ab} is the exchange integral and $\mathbf{S}_a$ and $\mathbf{S}_b$ are the spins of atoms a and b. The Hamiltonian yields states with energies

$$E = -J_{ab}[S(S + 1) - S_a(S_a + 1) - S_b(S_b + 1)]/2.$$

Here, $S_a = |\mathbf{S}_a|$ and $S_b = |\mathbf{S}_b|$. The spin quantum number for the a-b pair can take the values

$$S = |\mathbf{S}_a + \mathbf{S}_b|, |\mathbf{S}_a + \mathbf{S}_b - 1|, \ldots, |\mathbf{S}_a - \mathbf{S}_b|.$$

For the Mn^{2+}-Fe^{3+} pair, $S_a = S_b = 5/2$. The antiferromagnetic state has $S = 0$, whereas the ferromagnetic state has $S = 5$. Using the transition-state formalism (Slater, 1974; Ginsberg, 1980; Gubanov et al., 1983), it is possible to calculate the energy difference between the antiferromagnetic and ferromagnetic configurations and then estimate J. This gives $J = -1093$ cm^{-1}, implying that the coupling is strongly antiferromagnetic.

The lowest-energy optically induced $Mn^{2+} \rightarrow Fe^{3+}$ charge-transfer transition is from the Mn(e_g) to the Fe(t_{2g}) orbitals. Using the transition state formalism, this is calculated to be 14900 cm^{-1}. No evidence for such an absorption band in the spectra of minerals has been found. However, a band with this energy would be difficult to resolve from the bands due to ligand-field transitions of Mn^{2+} and Fe^{3+}. Even though such ligand-field transitions are nominally spin-forbidden, they are greatly intensified in solids because of the magnetic coupling between next-nearest-neighbor cations (e.g., Ferguson et al., 1966; Lohr, 1972; Rossman, 1975; Rossman, 1976).

Figure 4 shows the electronic structure of a $(Fe^{2+}Mn^{3+}O_{10})^{15-}$ cluster with Fe-O and Mn-O bond lengths of 2.21 and 2.01 Å, respectively. The electronic configuration corresponding to Fe^{2+} and Mn^{3+} cations is not that of the ground state, since the unoccupied spin-up Mn(e_g) orbital lies below the occupied spin-down Fe(t_{2g}) orbital. It follows that the Fe^{2+}-Mn^{3+} charge configuration is unstable. This is in accord with the EMF for the redox reaction

$$Mn^{3+} + Fe^{2+} = Mn^{2+} + Fe^{3+},$$

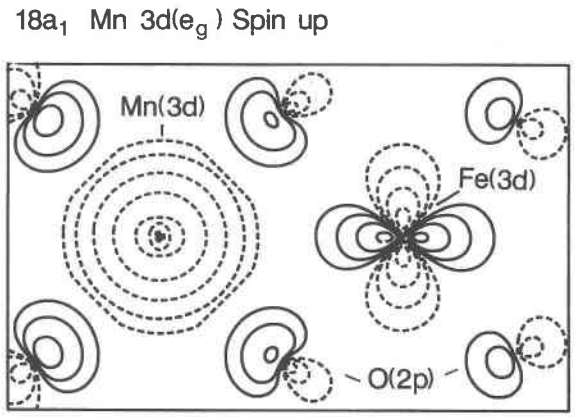

Fig. 3. Wave function contours for the highest occupied orbital in the antiferromagnetic $(FeMnO_{10})^{15-}$ cluster. This orbital is a Mn(e_g) d orbital (looking down the z axis), but there is a significant degree of electron delocalization via interaction with the $Fe^{3+}(t_{2g})$ d orbital. Note, however, that the contour lines are not equally spaced but are at 0.025, 0.05, 0.1, 0.2, 0.4, 0.8, and 1.6 (dashed contours are negative). Hence, only about 9% of the Mn $3d(e_g)$ electron is delocalized onto the Fe^{3+} cation. The Fe-Mn interaction through this orbital is antibonding and cancels out the effect of lower-energy Fe-Mn bonding orbitals. In the $(FeMnO_{10})^{15-}$ cluster, therefore, there is no net Fe-Mn bonding interaction.

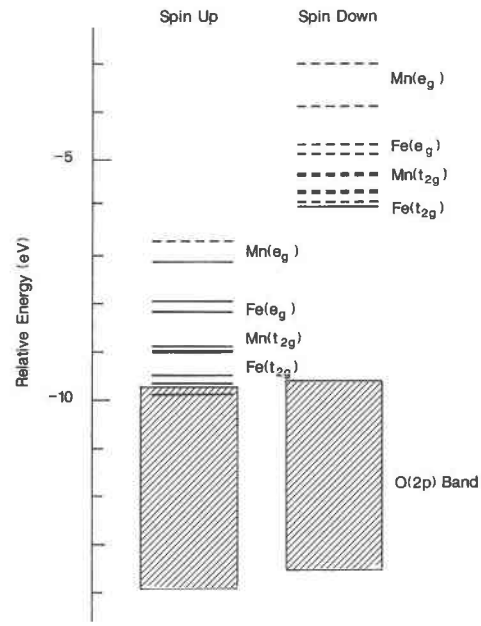

Fig. 4. Molecular orbital diagram for the charge configuration $Fe^{2+}Mn^{3+}O_{10}$. This is not a stable electronic configuration, since an occupied spin-down Fe(t_{2g}) orbital lies above an unoccupied spin-up Mn(e_g) orbital.

which, in acidic aqueous solution has $E^0 = 0.77$ V (Milazzo and Caroli, 1978). If the Mn site undergoes a strong tetragonal distortion, the occupied Mn(e_g) orbital may be sufficiently stabilized to allow the Mn^{3+}-Fe^{2+} configuration in the ground state. There does not appear to be any crystallographic evidence for Fe^{2+}-Mn^{3+} pairs in minerals. Such pairs might be indicated by optical absorption spectra, although the spectra of silicates containing both Fe and Mn are difficult to interpret. An important example is that of manganophyllite. Burns (1970) attributed absorption bands in manganophyllite to Mn^{3+} cations. This would imply the coexistence of Mn^{3+} and Fe^{2+}. Smith et al. (1983), however, assigned absorption bands in Mn-bearing phlogopites to octahedrally coordinated Mn^{2+} and octahedral or tetrahedrally coordinated Fe^{3+}. The calculations presented here support the assignment of bands in manganophyllite to the ligand-field transitions of Mn^{2+}, Fe^{2+}, and Fe^{3+}. Further study of the optical spectrum of manganophyllite may resolve absorption bands due to $Mn^{2+} \rightarrow Fe^{3+}$ charge transfer.

Fe^{3+}-Mn^{3+} interactions

The electronic structure of an $(FeMnO_{10})^{14-}$ cluster with Fe-O and Mn-O bond lengths of 2.01 Å is shown in Figures 5a and 5b. Both the ferromagnetic and antiferromagnetic spin configurations correspond to Fe^{3+}-Mn^{3+} charge configurations. In both the ferromagnetic and antiferromagnetic configurations, there is a net Fe-Mn bonding interaction that is presumably quite weak. A magnetic transition-state calculation was done to evaluate the sign and magnitude of the Fe^{3+}-Mn^{3+} magnetic coupling. The calculation predicts that the coupling will be antiferromagnetic with $J = -2104$ cm^{-1}. This is probably much greater than the actual value: coupling across edge-sharing polyhedra (90° superexchange) typically results in J values of 10–100 cm^{-1} (e.g., Goodenough, 1972).

The lowest energy charge-transfer transition is $Mn^{3+}(e_g) \rightarrow Fe^{3+}(t_{2g})$ and is calculated to be 17800 cm^{-1}. This energy would be a lower limit, however, since it assumes that the Mn^{3+} cation is in a nondistorted site. A tetragonal distortion via the Jahn-Teller effect of the Mn^{3+} site would destabilize the unoccupied $Mn^{3+}(e_g)$ orbital by as much as 4000 cm^{-1}, and this energy would have to be added to the charge-transfer energy. $Mn^{3+} \rightarrow Fe^{3+}$ charge transfer might, therefore, contribute to the visible region absorption edge in the spectra of Fe-Mn minerals. However, interference from the strong exchange-enhanced ligand-field bands of Fe^{3+} and the spin-allowed bands of Mn^{3+} would make resolution of $Mn^{3+} \rightarrow Fe^{3+}$ charge transfer difficult.

Conclusions

Some electron delocalization between Fe and Mn atoms is found in the Fe^{3+}-Mn^{3+} and Fe^{3+}-Mn^{2+} clusters and occurs through Mn(t_{2g})-Fe(e_g) and Mn(e_g)-Fe(t_{2g}) d-orbital overlap. In Fe^{3+}-Mn^{2+} pairs, however, the Fe-Mn bonding and antibonding interactions cancel out. The electron delocalization in the Fe-Mn clusters apparently does not induce ferromagnetic coupling via Zener's double-exchange mechanism. Both Fe^{3+}-Mn^{3+} and Fe^{3+}-Mn^{2+} cou-

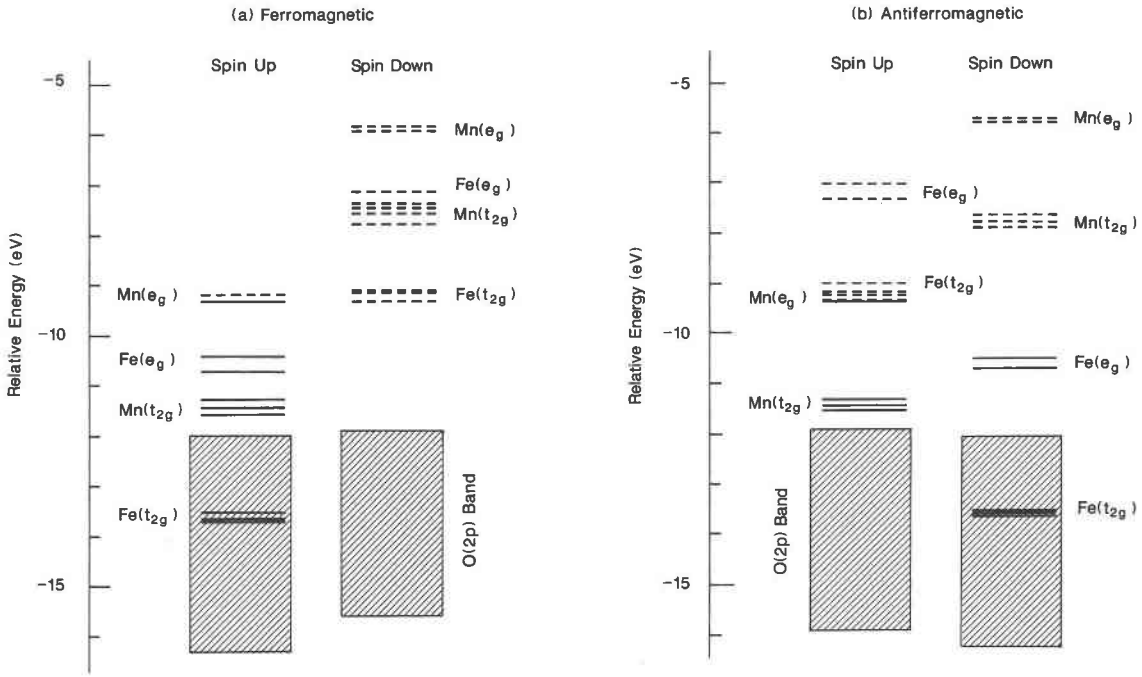

Fig. 5. Molecular orbital diagram for the $Fe^{3+}Mn^{3+}O_{10}$ cluster in the (a) ferromagnetic and (b) antiferromagnetic configurations.

pling across shared octahedral edges is antiferromagnetic via superexchange. Absorption bands due to optically induced $Mn^{2+} \rightarrow Fe^{3+}$ and $Mn^{3+} \rightarrow Fe^{3+}$ charge transfer should occur in the visible region spectra of minerals. However, neither Mn^{2+}-Fe^{3+} nor Mn^{3+}-Fe^{3+} charge-transfer bands may be easily resolved from the Fe and Mn ligand-field bands.

Acknowledgments

Helpful comments were provided by D. Williamson (Colorado School of Mines), A. Zunger (Solar Energy Research Institute), and an anonymous reviewer. Research on the quantum chemistry and spectroscopy of minerals is supported by the U.S. Geological Survey Development of Assessment Techniques program.

References cited

Burns, R.G. (1970) Mineralogical applications of crystal field theory. Cambridge University Press, Cambridge, England.

Coey, J.M.D., and Ghose, S. (1988) Magnetic phase transitions in silicate minerals. In S. Ghose, J.M.D. Coey, and E. Salje, Eds., Structural and magnetic phase transitions in minerals, pp. 162–184. Springer-Verlag, New York.

Ferguson, J., Guggenheim, H.J., and Tanabe, Y. (1966) The effects of exchange interactions on the spectra of octahedral manganese(II) compounds. Journal of the Physical Society of Japan, 21, 347–354.

Ginsberg, A.P. (1980) Magnetic exchange in transition metal complexes: 12. Calculation of cluster exchange coupling constants with the Xα–scattered wave method. Journal of the American Chemical Society, 102, 111–117.

Goodenough, J.B. (1972) Metallic oxides. Progress in Solid State Chemistry, 5, 1–399.

Gubanov, V.A., Liechtenstein, A.I., and Postnikov, A.V. (1983) Cluster Xα approach to magnetic interactions and phase transitions in solids. International Journal of Quantum Chemistry, 23, 1517–1528.

Johnson, K.H. (1973) Scattered wave theory of the chemical bond. Advances in Quantum Chemistry, 7, 576–580.

Lohr, L.L. (1972) Spin-forbidden electronic excitations in transition metal complexes. Coordination Chemistry Reviews, 8, 241–259.

Milazzo, G., and Caroli, S. (1978) Tables of standard electrode potentials. Wiley, New York.

Norman, J.G. (1976) Non-empirical versus empirical choices for overlapping sphere radii ratios in SCF-Xα-SW calculations on ClO_4^- and SO_2. Molecular Physics, 31, 1191–1198.

Rossman, G.R. (1975) Spectroscopic and magnetic studies of ferric iron hydroxy sulphates: Intensification of color in ferric iron clusters bridged by a single hydroxide ion. American Mineralogist, 60, 698–704.

——— (1976) Spectroscopic characteristics and magnetic studies of ferric iron hydroxy sulphates—the series $Fe(OH)SO_4 \cdot nH_2O$ and the jarosites. American Mineralogist, 61, 398–404.

Schwarz, K. (1972) Optimization of the statistical exchange parameter α for the free ions H through Nb. Physical Review B, 5, 2466–2468.

Shannon, R.D., and Prewitt, C.T. (1969) Effective ionic radii in oxides and fluorides. Acta Crystallographica, B25, 925–946.

Sherman, D.M. (1984) The electronic structures of manganese oxide minerals. American Mineralogist, 69, 788–799.

——— (1985) The electronic structures of Fe^{3+} coordination sites in iron oxides; Applications to spectra, bonding and magnetism. Physics and Chemistry of Minerals, 12, 161–175.

——— (1987a) Molecular orbital (SCF-Xα-SW) theory of metal-metal charge transfer processes in minerals: I. Application of Fe^{2+}-Fe^{3+} charge transfer and "electron delocalization" in mixed-valence iron oxides and silicates. Physics and Chemistry of Minerals, 14, 355–363.

——— (1987b) Molecular orbital (SCF-Xα-SW) theory of metal-metal charge transfer processes in minerals: II. Application to Fe^{2+}-Ti^{4+} charge transfer in oxides and silicates. Physics and Chemistry of Minerals, 14, 364–367.

Slater, J.C. (1974) The self-consistent field for molecules and solids, Vol. 4. In Quantum theory of molecules and solids, 583 p. McGraw-Hill, New York.

Smith, G., Hålenius, U., Annersten, H., and Ackermann, L. (1983) Optical and Mössbauer spectra of manganese-bearing phlogopites: Fe^{3+}_{IV}-Mn^{2+}_{VI} pair absorption as the origin of reverse pleochroism. American Mineralogist, 68, 759–768.

Vandenberghe, R.E., Verbeeck, A.E., de Grave, E., and Stiers, W. (1986) ^{57}Fe Mössbauer effect study of Mn-substituted goethite and hematite. Hyperfine Interactions, 29, 1157–1160.

Manuscript received August 12, 1989
Manuscript accepted December 2, 1989